Research Square

Preprints are preliminary reports that have not undergone peer review.
They should not be considered conclusive, used to inform clinical practice,
or referenced by the media as validated information.

Targeting RNF8 Effectively Reverse Cisplatin and Doxorubicin Resistance in Endometrial Cancer

Ben Yang
China-Japan Union Hospital of Jilin University
Wang Ke
China-Japan Union Hospital of Jilin University
Yingchun Wan
China-Japan Union Hospital of Jilin University
Tao Li (lt606403@jlu.edu.cn)
China-Japan Union Hospital of Jilin University https://orcid.org/0000-0002-6981-2977

Primary research

Keywords: Endometrial cancer, RNF8, cisplatin, doxorubicin, resistance

Posted Date: September 2nd, 2020

DOI: https://doi.org/10.21203/rs.3.rs-57263/v1

License: This work is licensed under a Creative Commons Attribution 4.0 International License.
Read Full License

Version of Record: A version of this preprint was published at Biochemical and Biophysical Research Communications on March 1st, 2021. See the published version at https://doi.org/10.1016/j.bbrc.2021.01.046.

Abstract

Background

Endometrial cancer (EC) is one of the most frequent gynecological malignancy worldwide. However, resistance to chemotherapy remains one of the major difficulties in the treatment of EC. Thus, there is an urgent requirement to understand mechanisms of chemoresistance and identify novel regimens for patients with EC.

Methods

Cisplatin and doxorubicin resistant cell lines were acquired by continuous exposing parental EC cells to cisplatin or doxorubicin for 3 months. Cell viability was determined by using MTT assay. Protein Expression levels of protein were examined by western blotting assay. mRNA levels were measured by quantitative polymerase chain reaction (qPCR) assay. Ring finger protein 8 (RNF8) knockout cell lines were generated by clustered regularly interspaced short palindromic repeats (CRISPR)–Cas9 gene editing assay. Nonhomologous end joining (NHEJ) efficiency were quantified by plasmid based NHEJ assay. DNA double strand breaks (DSB) were generated using laser micro-irradiation. Protein recruitment to DSB was analyzed by immunofluorescent assay. Tumor growth was examined by AN3CA xenograft mice model.

Results

We found that protein and mRNA expression levels of RNF8 were significantly increased in both cisplatin and doxorubicin resistant EC cells. Cell survival assay showed that RNF deficiency significantly enhanced the sensitivity of resistant EC cells to cisplatin and doxorubicin ($P < 0.01$). In addition, chemoresistant EC cells exhibited increased NHEJ efficiency. Knockout of RNF8 in chemoresistant EC cells significantly reduced NHEJ efficiency and prolonged Ku80 retention on DSB. Moreover, cisplatin resistant AN3CA xenograft showed that RNF8 deficiency overcame cisplatin resistance.

Conclusions

Our *in vitro* and *in vivo* assays provide evidence for RNF8, which is a NHEJ factor, serving as a promising, novel target in EC chemotherapy.

Background

Endometrial cancer (EC) is one of the most common gynecological malignancy [1, 2], with estimated 65, 620 new cases and 12, 590 endometrial cancer deaths in 2020. The prognosis of early stage endometrial cancer is good. However, more than 25% of patients are diagnosed at advanced stage with invasive

primary tumor and subsequently accompanied by metastases [3]. The survival rate of these patients is less than 20% albeit of aggressive treatment, largely due to resistance to chemotherapy [4]. Therefore, it is critical to elucidate the mechanisms of chemoresistance in EC and identify novel methods to improve EC therapy. The current and most frequently used chemotherapeutic drugs for patients with poor outcome include cisplatin, doxorubicin and taxanes [3, 5]. Cisplatin and doxorubicin are DNA damaging agents targeting DNA replication and topoisomerase II respectively [6, 7]. Both generate DNA double strand breaks (DSB) that leads to cell death. Thus, abnormal DSB repair is one of the plausible mechanisms for resistance to cisplatin and doxorubicin.

DSB is highly toxic and probably the most dangerous of the many types of DNA damage. Unrepaired DSB results in cell death, while misrepaired DSBs can cause translocations [8]. Human cells developed two major DSB repair pathways, homologous recombination (HR) and non-homologous end joining (NHEJ) [8, 9]. Each of them requires key factors and leads to different DSB repair outcomes. HR is considered to be the ‘error-free’ pathway as it incorporates sister chromatids as a template to guide polymerization. Hence, HR is restricted to the S and G2 phase of the cell cycle when sister chromatids are available [10], while NHEJ is active throughout the cell cycle due to the independence of a template [11]. NHEJ is a relatively simple and ‘error-prone’ DSB repair pathway. The first step of NHEJ is DNA binding by Ku70/80 heterodimer, which then recruits the catalytic subunit of the DNA dependent protein kinase (DNA-PKcs) [12]. Ligation of the DSB requires compatible DNA ends that can be trimmed by DNA end processing factors, such as Artemis, polynucleotide kinase-phosphatase (PNKP), Tyrosyl-DNA phosphodiesterase 1 (TDP1) and Werner syndrome protein (WRN) [13–16]. If necessary, the gap between DNA ends will be filled by the polymerase X family, such as such as Polμ or Polλ [17]. Finally, the compatible DNA ends are ligated by X-ray cross-complementation group 4 (XRCC4), Xrcc4 like factor (XLF) and DNA ligase IV [18, 19].

RNF8 was identified in 2007 as a novel E3 ubiquitin ligase that acts in the DNA signaling pathway [20–22]. Recent study found that RNF8 is required for efficient NHEJ by regulating abundance of Ku80 at DNA damage site. Increased expression of Ku80 is correlated with radioresistance and cisplatin resistance in rectal carcinoma and lung adenocarcinoma patients respectively [23–25]. Hence, inhibition of Ku80 is a potential strategy to overcome radio- and chemoresistance. However, Ku80 is essential for NHEJ and Ku80 depletion results in defective lymphocyte development, atrophic skin and hair follicles, osteopenia, premature growth plate closure, hepatocellular degeneration, and shortened life span [26, 27]. To avoid high toxicity of NHEJ depletion, we thought to inhibit NHEJ regulating factor RNF8 to provide improved sensitivity to DNA damaging agents. Our study found that RNF8 contributes to increased NHEJ efficiency in cisplatin and doxorubicin resistant EC cells. Importantly, RNF8 deficiency significantly sensitize resistant EC *in vitro* and *in vivo*, indicating that RNF8 is a promising target for advanced EC treatments.

Material And Methods

Cell lines and reagents

Ishikawa (Sigma-Aldrich; Merck KGaA) and AN3CA (American Tissue Culture Collection) cells were cultured at 37˚C in a humidified incubator with 5% CO_2 in Eagle's Minimum Essential Medium with 10% FBS for <3 weeks.

Cisplatin resistant Ishikawa and AN3CA cells were generated by incubating WT cells in medium with 2.5 μM cisplatin for 4 weeks, subsequently followed by 5 and 10 μM cisplatin for 4 weeks at each concentration. Doxorubicin resistant Ishikawa and AN3CA cells were generated by incubating WT cells in medium with 0.5 μM doxorubicin for 4 weeks, subsequently followed by 1 and 2 μM doxorubicin for 4 weeks at each concentration.

Cisplatin and doxorubicin were purchased from Sigma-Aldrich.

Analysis of cell viability

EC were seeded in 96-well plates at a density of $5x10^3$ cells/well in triplicate. After 24 h, cells were treated with cisplatin or doxorubicin for 48 h and the cell viability was measured using MTT assay. Briefly, 10 μl MTT (Sigma-Aldrich; Merck KGaA) solution was added to each well, and the plates were incubated for 2.5 h at 37˚C. The absorbance was measured at 490 nm using a Microplate spectrophotometer (BioTek Instruments, Inc.).

NHEJ reporter assay

A total of 10 μg of NHEJ reporter plasmid was linearized using NheI and purified using the QIAquick Gel Extraction kit according to the manufacturer's instructions (Qiagen Corporation). 1 μg of purified plasmid was transfected into EC cells using Lipofectamine® 2000 according to the manufacturer's protocols (Thermo Fisher Scientific, Inc.). Cells with chromosomally integrated reporter were selected by incubating in medium with 1 mg/ml geneticin for 2 weeks. To measure NHEJ efficiency, stable reporter cells were seeded at $2x10^5$ cells/ml in a 6-well plate and allow attachment for 24 h. To start the NHEJ, 1 μg of I-SceI plasmid was transfected into stable reporter cells. Cells were incubated for 48 to generate DSB and repair. Cells were harvested and green fluorescent protein (GFP) positive cells, which indicate successful DSB repair, were count using BD FACSCelesta™ Flow Cytometer (BD Biosciences).

Reverse transcription-quantitative PCR (RT-qPCR)

Total RNA was extracted using the RNeasy Mini Kit (Qiagen Corporation) and was reverse transcribed using the TaqMan™ Reverse Transcription Reagents (ThermoFisher Scientific). Subsequently the Fast SYBR™ Green Master Mix (ThermoFisher Scientific) was used for qPCR to detect the mRNA levels of RNF8, according to the manufacturer's instructions using a Real-Time PCR system (Eppendorf Thermal Cycler Eco; Eppendorf). The following primers were used: RNF8 forward, 5'-ATTAAGTTGCGCGAGAGGAA-3' and reverse, 5'-AGCTCGTTCTCCAGCAAGTC-3'; GAPDH forward, 5'-GTCTCCTCTGACTTCAACAGCG-3' and reverse, 5'-ACCACCCTGTTGCTGTAGCCAA-3'

Studies involving patient samples were approved by the China-Japan Union Hospital of Jilin University, and all patients provided informed consent, in accordance with the Declaration of Helsinki.

CRISPR-Cas9-mediated RNF8 deletion

A pool of 3 plasmids encoding Cas9 coding gene and RNF8 guide RNA (cat. no. sc-401909; Santa Crus Biotechnology, Inc.) or CRISPR/Cas9-Ctr Plasmid (cat. no. sc-418922; Santa Crus Biotechnology, Inc.) was transfected into AN3CA Cis-R and AN3CA Dox-R cells using Lipofectamine® 2000. Cells were harvested and seeded in 96-well plate at densities of 100, 200 and 300 cells/ml and incubated for 2 weeks or until single colonies form in each well. Single clones were picked and expanded. RNF8 expression was assayed using western blot analysis with RNF8 antibody (cat. no. sc-271462; Santa Crus Biotechnology, Inc). 2 RNF8 KO clones were randomly picked for further studies.

Western blot analysis

Cells were pelleted, resuspend and vortexed in RIPA lysis buffer (50 mM Tris-HCl, pH 8, 150 mM NaCl, 1% NP40). Cell lysate was centrifuged for 20 minutes at 12,000 x rpm at 4°C and the supernatant was retained, following which the protein concentration of the lysate was determined. Cell lysate samples were denatured using SDS-PAGE sample buffer and separated using SDS-PAGE. Separated samples were transferred to nitrocellulose membrane (BioRad Laboratories, Inc.). Membrane was blocked with 3% BSA in 1X PBST buffer (1xPBS with 0.1% Tween-20). The membrane was ten incubated with primary antibodies followed by incubation with horseradish peroxidase-conjugated secondary antibodies. The protein signals were detected using an enhanced chemiluminescence reagent (Thermo Fisher Scientific, Inc.) and the proteins were visualized using the SuperSignalTM west pico PLUS Chemiluminescent Substrate (ThermoFisher Scientific, Inc.). The following antibodies were used: anti-actin (cat. no. 3700; Cell Signaling Technology, Inc.), anti-Ku80 (Cell Signaling Technology, Inc.), anti-RNF8 (cat. no. sc-271462; Santa Crus Biotechnology, Inc).

Laser microirradiation and Immunofluorescence staining

AN3CA Cis-R cells were seeded at $3x10^5$ cells/ml on glass-bottomed culture dishes (MatTek Corporation), following which cells were stained with Hoechst33342 (10μg/ml) for 1 h. Cells were then exposed for 15 s to the 405 nm laser microbeam with a Micropoint Ablation System (Photonics Instruments, St. Charles, IL, USA), which is focused by a 60x oil immersion inverted microscope objective. Cells were then incubated at 37˚C in a humidified incubator with 5% CO_2 for 4 h. After washing with PBS, cells were fixed with 4% paraformaldehyde for 10 min and permeabilized in 0.5% triton X-100 solution for 5 min at room temperature. Cells were blocked with 3% BSA in wash buffer (1xPBS with 0.02% Tween-20) for 30 min and incubated with primary antibody for 2 h. Subsequently, samples were washed with wash buffer and incubated with secondary antibody for 45 min. Nuclear DNA was stained with DAPI staining solution. The coverslips were mounted, and signals were visualized by a fluorescence microscope (Nikon ECLIPSE E800).

Animals

All the animal experiments were authorized by the Laboratory Animal Care and Ethical Committee of the China-Japan Union Hospital of Jilin University, and were performed following the Guide for the Care and Use of Laboratory Animals (8th edition, 2011, National Academies Press (US)).

BALB/c nude mice (female, 4-week-old, 18 ± 2 g) were purchased from Charles river (Beijing, China). $5x10^6$ AN3CA Cis-R or AN3CA Cis-R-KO cells were subcutaneously injected in the right flank to generate tumor xenograft model. Tumor size was assessed by measuring tumor diameters with Vernier calipers twice a week. Tumor volume is calculated according to the formula, volume=length x $width^2/2$. Treatments were given when the tumors were approximately 100 mm^3 in volume. Mice were treated with vehicle or cisplatin (8 mg/kg/3 day) intraperitoneally for 2 weeks. Tumor volume and body weight were measured every 3 days for 3 weeks.

Statistical analysis

GraphPad software (Prism; v7.0) was used to create and analyze all the graphs. A Student's t-test was used for comparison of two groups. A one-way or two-way ANOVA analysis with a Bonferroni post-test was used to compare multiple groups. $P<0.05$ was indicated to indicate a statistically significant difference.

Results

Expression of RNF8 is increased in cisplatin and doxorubicin resistant EC cells

To determine whether RNF8 is correlated with chemoresistance in EC, we established cisplatin resistant Ishikawa (ISH-Cis-R), AN3CA (AN3CA-Cis-R), doxorubicin resistant Ishikawa (ISH-Dox-R), and AN3CA (AN3CA-Dox-R) cell lines. As shown in Fig. 1a and b, we successfully increased cisplatin IC_{50} by 3.21- and 3,98-fold in Ishikawa and AN3CA cell lines respectively. Similarly, doxorubicin resistant Ishikawa and AN3CA cell lines exhibited 4 to 7 folds IC_{50} as compared to their parental cell lines (Fig. 1c and d).

To measure RNF8 expression, we next extracted RNA from chemoresistant cells and their parental cells. mRNA levels of RNF8 was measured using qPCR and we found that RNF8 was significantly increased in resistant cell lines as compare to that in WT cell lines (Fig. 1e to h). Consistently, the protein levels of RNF8 in these 4 pairs of EC cell lines showed that RNF8 is overexpressed in resistant cell lines. (Fig. 1i). We also collected samples from platinum sensitive and resistant patient to verify clinical relevance of RNF8 in EC. Indeed, we found that RNF8 was significantly increased in patients resistant to platinum drugs as compared to that in platinum-sensitive patients (Fig. 1j), suggesting expression of RNF8 is positively correlated with cisplatin and doxorubicin resistance in EC.

Depletion of RNF8 sensitize cisplatin and doxorubicin resistant EC cells

We then validated whether RNF8 is a potential target to improve cisplatin or doxorubicin resistance. With the convenience of commercially available CRISPR/cas9 RNF8 plasmid, RNF8 deficient AN3CA-Cis-R and AN3CA-Dox-R cells (AN3CA-Cis-R-KO1, AN3CA-Cis-R-KO2, AN3CA-Dox-R-KO1 and AN3CA-Dox-R-KO2) were generated. The western blot analysis of RNF8 showed no detectable RNF8 protein expression in the KO cell lines as compared to that in their parental cell lines treated with control CRISPR plasmid (Fig. 2a and b).

Subsequently, cell viability was measured against cisplatin and doxorubicin. As shown in Fig. 2c and d, RNF8 knockout resistant cell lines were more sensitive to cisplatin and doxorubicin compared with that in AN3CA-Cis-R-Ctr and AN3CA-Dox-R-Ctr cells. To eliminate off target effect caused by transfection of CRISPR plasmid, we ectopically expressed RNF8 in KO cells (Fig. 2a and b). We found that complementation of RNF8 restored cisplatin and doxorubicin resistance (Fig. 2c and d), suggesting RNF8 deficiency indeed overcomes chemoresistance in EC.

RNF8 deficiency reduces NHEJ efficiency in cisplatin and doxorubicin resistant EC cells

RNF8 is a novel NHEJ factor that orchestrates NHEJ pathway. Therefore, we hypothesize that elevated RNF8 expression leads to increase of NHEJ efficiency. We compared NHEJ events in AN3CA, AN3CA-Cis-R and AN3CA-Dox-R cell lines and observed that AN3CA-Cis-R and AN3CA-Dox-R showed 2.81-fold and 3.68-fold NHEJ events compared to AN3CA cells respectively (Fig. 3a and b). In the absence of RNF8, NHEJ efficiency of AN3CA-Cis-R cells reduced to a similar level in WT cells, and RNF8 expression in KO cells rescued NHEJ efficiency (Fig. 3a and b).

Recent study found that RNF8 affect NHEJ by affecting Ku80-DNA binding. To elucidate the role of RNF8 in NHEJ in resistant EC cells, we generated DSB using microirradiation and observed Ku80 retention at DSB site after 4 h of recovery in AN3CA-Cis-R and AN3CA-Cis-R-KO cells. As shown in Fig. 3c, RNF8 deficiency resulted in prolonged retention of Ku80 at DNA damage site. Similar results were found in AN3CA-Dox-R and AN3CA-Dox-R-KO cells (Fig. 3d). These results suggesting that increased RNF8 improves NHEJ by keeping pool of free Ku80 in resistant EC cells.

Inhibition of RNF8 increases sensitivity to cisplatin *in vivo*

To further validated the effect of RNF8 depletion on cisplatin sensitivity in EC, we measured tumor growth in response to cisplatin using AN3CA-Cis-R-Ctr and AN3CA-Cis-R-KO1 xenograft models. The AN3CA-Cis-R-Ctr and AN3CA-Cis-R-KO1 cells were subcutaneously implanted in female nude mice, and the cisplatin treatment was started when the tumor volume reached 100mm^3. We treated the mice with cisplatin (8 mg/kg/3 day) for 3 weeks and we found that AN3CA-Cis-R-Ctr group did not significantly respond to cisplatin (Fig. 4a and b). In consistent with the *in vitro* cell based assay, combination of RNF8 deficiency and cisplatin resulted in very promising synergy in suppression of tumor growth without detectable toxicity (Fig. 4a-d). We also noted that AN3CA-Cis-R-Ctr and AN3CA-Cis-R-KO1 groups had no significant difference in tumor volume without cisplatin treatment, indicating RNF8 deficiency alone does not affect tumor growth.

Together our data suggest that RNF8 is a potential target and inhibition of RNF8 is a promising strategy to overcome cisplatin and doxorubicin resistance in EC patients.

Discussion

Despite the advances in surgery, chemotherapy, radiation therapy and hormone therapy, treatment of EC remains a clinical and scientific challenge. One of the critical obstacles is resistance to current chemotherapeutical drugs. Therefore, understanding mechanism of chemoresistance is essential to develop novel approaches for EC treatment.

Cisplatin has been used as broad-spectrum antitumor compound since 1970s. It crosslinks DNA and forms DNA-platinum nonfunctional adducts that result in cell cycle arrest and apoptosis [28]. DSBs are formed by processing DNA interstrand crosslinks during replication [29]. Therefore, impaired DSB repair accumulates breaks in replicating cancer cells and improves inhibition of tumor growth by cisplatin. Doxorubicin also generates DSBs by stabilizing the topoisomerase II-DNA complex after it has cleaved DNA double strands during replication, thereby ceasing replication [7]. Since cisplatin and doxorubicin share a common mechanism of action, inhibition of NHEJ, which is the most commonly used and efficient DSB repair pathway, is a potential strategy for overcoming cisplatin and doxorubicin resistance. Moreover, NHEJ is the major DSB repair pathway for ionizing radiation induced DNA damage [30]. Thus, inhibition of NHEJ may also benefit EC patients suffering from radioresistance. Most well studied NHEJ inhibitors include DNA-PKcs inhibitors (AZD7648, NU7026 and VX-984) and DNA ligase IV inhibitor SCR7, which was then proved not potent [31–34]. Because NHEJ is an essential pathway maintaining genome integrity, depletion of NHEJ by inhibiting its core factors may result in less selectivity to cancer cells and cause severe side effects. Therefore, this study focused on identification of a NHEJ factor altered in chemoresistance.

NHEJ is initiated by DNA binding of a ring shaped Ku70/80 heterodimer, which must be removed upon completion of repair. Yeast study suggested that Ku escapes DNA after nicking DNA strand [35]. Another mechanism involves ubiquitination and proteasomal degradation of Ku from intact DNA strands that requires E3 ligase RNF8 [36]. Depletion of RNF8 retains Ku80 on DNA and impairs NHEJ efficiency [36]. Recent study found that RNF8 facilities doxorubicin resistance in cancer stem cells [37]and radiation resistance in nasopharyngeal cancer, bladder cancer [38, 39]. These studies prompt us to investigate the role of RNF8 in NHEJ in EC. Our study found that inhibition of RNF8 decreases NHEJ efficiency, but does not deplete NHEJ, in cisplatin and doxorubicin resistant EC cells. Importantly, we did not observe cellular toxicity nor loss of body weight in mice result from RNF8 inhibition, suggesting RNF8 is a promising and target for overcoming chemoresistance in EC. However, no potent RNF8 inhibitor has been developed yet. The E3 ligase enzymatic activity of RNF8 allows us to use high-throughput screening to identify small molecules that disrupt enzyme-substrate interaction or inhibit generation of product.

Conclusion

In this study, we demonstrated the role of RNF8 in resistance to cisplatin and doxorubicin, which are most commonly used chemotherapeutic regimens in EC. RNF8 expression is positively correlated with cisplatin and doxorubicin resistance in EC patients and in EC cell lines. We further showed that RNF8 deficiency generates great improvement of sensitivity to cisplatin and doxorubicin in resistant EC cell lines. Mechanistically, we found that depletion of RNF8 restrain Ku80 at the DSB site and impaired efficiency NHEJ. Our study suggests that RNF8 may serve as a promising target for advanced EC treatment.

Abbreviations

EC
Endometrial cancer
RNF8
Ring finger protein 8
DSB
DNA double strand breaks
HR
Homologous recombination
NHEJ
Nonhomologous end joining
PNKP
Polynucleotide kinase-phosphatase
TDP1
Tyrosyl-DNA phosphodiesterase 1
WRN
Werner syndrome protein
XRCC4
X-ray cross-complementation group 4
XLF
Xrcc4 like factor
KO
Knockout

Declarations

Availability of data and materials

All data generated or analyzed in this study are included in this published article.

Funding

Not applicable.

Corresponding authors

Correspondence to Yingchun Wan or Tao Li

Contributions

BY, YW and TL contributed to conception and design. BY and WK carried out analysis and wrote the paper. WK collected and processed the data. YW and TL edited the paper and provided constructive comments. All authors read and approved the final manuscript.

Ethics declarations

Ethics approval and consent to participate

Not applicable.

Consent for publication

Not applicable.

Competing interests

The authors declare no conflict of interest.

Acknowledgements

Not applicable.

References

1. Smith RA, von Eschenbach AC, Wender R, Levin B, Byers T, Rothenberger D, Brooks D, Creasman W, Cohen C, Runowicz C, et al. American Cancer Society guidelines for the early detection of cancer: update of early detection guidelines for prostate, colorectal, and endometrial cancers. Also: update 2001–testing for early lung cancer detection. Cancer J Clin. 2001;51(1):38–75. quiz 77–80.
2. Cramer DW. The epidemiology of endometrial and ovarian cancer. Hematol Oncol Clin N Am. 2012;26(1):1–12.
3. Colombo N, Preti E, Landoni F, Carinelli S, Colombo A, Marini C, Sessa C, Group EGW: **Endometrial cancer**: **ESMO Clinical Practice Guidelines for diagnosis**, **treatment and follow-up**. *Annals of oncology: official journal of the European Society for Medical Oncology* 2013, **24 Suppl 6**:vi33-38.
4. Casciato DA, Territo MC. Manual of clinical oncology. 7th ed. Philadelphia: Wolters Kluwer/Lippincott Williams & Wilkins Health; 2012.
5. Lalwani N, Prasad SR, Vikram R, Shanbhogue AK, Huettner PC, Fasih N. Histologic, molecular, and cytogenetic features of ovarian cancers: implications for diagnosis and treatment. Radiographics: a

review publication of the Radiological Society of North America Inc. 2011;31(3):625–46.
6. Wang D, Lippard SJ. Cellular processing of platinum anticancer drugs. Nature reviews Drug discovery. 2005;4(4):307–20.
7. Thorn CF, Oshiro C, Marsh S, Hernandez-Boussard T, McLeod H, Klein TE, Altman RB. Doxorubicin pathways: pharmacodynamics and adverse effects. Pharmacogenet Genomics. 2011;21(7):440–6.
8. Jeggo PA, Lobrich M. DNA double-strand breaks: their cellular and clinical impact? Oncogene. 2007;26(56):7717–9.
9. Haber JE. Partners and pathwaysrepairing a double-strand break. Trends Genet. 2000;16(6):259–64.
10. Hinz JM, Yamada NA, Salazar EP, Tebbs RS, Thompson LH. Influence of double-strand-break repair pathways on radiosensitivity throughout the cell cycle in CHO cells. DNA Repair. 2005;4(7):782–92.
11. Rothkamm K, Kruger I, Thompson LH, Lobrich M. Pathways of DNA double-strand break repair during the mammalian cell cycle. Molecular cellular biology. 2003;23(16):5706–15.
12. Lee SE, Mitchell RA, Cheng A, Hendrickson EA. Evidence for DNA-PK-dependent and -independent DNA double-strand break repair pathways in mammalian cells as a function of the cell cycle. Molecular cellular biology. 1997;17(3):1425–33.
13. Ma Y, Pannicke U, Schwarz K, Lieber MR. Hairpin opening and overhang processing by an Artemis/DNA-dependent protein kinase complex in nonhomologous end joining and V(D)J recombination. Cell. 2002;108(6):781–94.
14. Bernstein NK, Williams RS, Rakovszky ML, Cui D, Green R, Karimi-Busheri F, Mani RS, Galicia S, Koch CA, Cass CE, et al. The molecular architecture of the mammalian DNA repair enzyme, polynucleotide kinase. Molecular cell. 2005;17(5):657–70.
15. Li J, Summerlin M, Nitiss KC, Nitiss JL, Hanakahi LA. TDP1 is required for efficient non-homologous end joining in human cells. DNA Repair. 2017;60:40–9.
16. Perry JJ, Yannone SM, Holden LG, Hitomi C, Asaithamby A, Han S, Cooper PK, Chen DJ, Tainer JA. WRN exonuclease structure and molecular mechanism imply an editing role in DNA end processing. Nat Struct Mol Biol. 2006;13(5):414–22.
17. Lieber MR. The mechanism of double-strand DNA break repair by the nonhomologous DNA end-joining pathway. Annual review of biochemistry. 2010;79:181–211.
18. Ahnesorg P, Smith P, Jackson SP. XLF interacts with the XRCC4-DNA ligase IV complex to promote DNA nonhomologous end-joining. Cell. 2006;124(2):301–13.
19. Buck D, Malivert L, de Chasseval R, Barraud A, Fondaneche MC, Sanal O, Plebani A, Stephan JL, Hufnagel M, le Deist F, et al. Cernunnos, a novel nonhomologous end-joining factor, is mutated in human immunodeficiency with microcephaly. Cell. 2006;124(2):287–99.
20. Huen MS, Grant R, Manke I, Minn K, Yu X, Yaffe MB, Chen J. RNF8 transduces the DNA-damage signal via histone ubiquitylation and checkpoint protein assembly. Cell. 2007;131(5):901–14.
21. Kolas NK, Chapman JR, Nakada S, Ylanko J, Chahwan R, Sweeney FD, Panier S, Mendez M, Wildenhain J, Thomson TM, et al. Orchestration of the DNA-damage response by the RNF8 ubiquitin

ligase. Science. 2007;318(5856):1637–40.

22. Mailand N, Bekker-Jensen S, Faustrup H, Melander F, Bartek J, Lukas C, Lukas J. RNF8 ubiquitylates histones at DNA double-strand breaks and promotes assembly of repair proteins. Cell. 2007;131(5):887–900.
23. Shang B, Jia Y, Chen G, Wang Z. Ku80 correlates with neoadjuvant chemotherapy resistance in human lung adenocarcinoma, but reduces cisplatin/pemetrexed-induced apoptosis in A549 cells. Respiratory research. 2017;18(1):56.
24. Komuro Y, Watanabe T, Hosoi Y, Matsumoto Y, Nakagawa K, Tsuno N, Kazama S, Kitayama J, Suzuki N, Nagawa H. The expression pattern of Ku correlates with tumor radiosensitivity and disease free survival in patients with rectal carcinoma. Cancer. 2002;95(6):1199–205.
25. Ma Q, Li P, Xu M, Yin J, Su Z, Li W, Zhang J. Ku80 is highly expressed in lung adenocarcinoma and promotes cisplatin resistance. Journal of experimental clinical cancer research: CR. 2012;31:99.
26. Vogel H, Lim DS, Karsenty G, Finegold M, Hasty P. Deletion of Ku86 causes early onset of senescence in mice. Proc Natl Acad Sci USA. 1999;96(19):10770–5.
27. Gu Y, Seidl KJ, Rathbun GA, Zhu C, Manis JP, van der Stoep N, Davidson L, Cheng HL, Sekiguchi JM, Frank K, et al. Growth retardation and leaky SCID phenotype of Ku70-deficient mice. Immunity. 1997;7(5):653–65.
28. Dasari S, Tchounwou PB. Cisplatin in cancer therapy: molecular mechanisms of action. Eur J Pharmacol. 2014;740:364–78.
29. Frankenberg-Schwager M, Kirchermeier D, Greif G, Baer K, Becker M, Frankenberg D. Cisplatin-mediated DNA double-strand breaks in replicating but not in quiescent cells of the yeast Saccharomyces cerevisiae. Toxicology. 2005;212(2–3):175–84.
30. Toulany M. **Targeting DNA Double-Strand Break Repair Pathways to Improve Radiotherapy Response**. *Genes* 2019, 10(1).
31. Riballo E, Critchlow SE, Teo SH, Doherty AJ, Priestley A, Broughton B, Kysela B, Beamish H, Plowman N, Arlett CF, et al. Identification of a defect in DNA ligase IV in a radiosensitive leukaemia patient. Current biology: CB. 1999;9(13):699–702.
32. Srivastava M, Nambiar M, Sharma S, Karki SS, Goldsmith G, Hegde M, Kumar S, Pandey M, Singh RK, Ray P, et al. An inhibitor of nonhomologous end-joining abrogates double-strand break repair and impedes cancer progression. Cell. 2012;151(7):1474–87.
33. Hu Z, Shi Z, Guo X, Jiang B, Wang G, Luo D, Chen Y, Zhu YS. Ligase IV inhibitor SCR7 enhances gene editing directed by CRISPR-Cas9 and ssODN in human cancer cells. Cell bioscience. 2018;8:12.
34. Greco GE, Matsumoto Y, Brooks RC, Lu Z, Lieber MR, Tomkinson AE. SCR7 is neither a selective nor a potent inhibitor of human DNA ligase IV. DNA Repair. 2016;43:18–23.
35. Wu D, Topper LM, Wilson TE. Recruitment and dissociation of nonhomologous end joining proteins at a DNA double-strand break in Saccharomyces cerevisiae. Genetics. 2008;178(3):1237–49.

36. Feng L, Chen J. The E3 ligase RNF8 regulates KU80 removal and NHEJ repair. Nat Struct Mol Biol. 2012;19(2):201–6.
37. Lee HJ, Li CF, Ruan D, Powers S, Thompson PA, Frohman MA, Chan CH. The DNA Damage Transducer RNF8 Facilitates Cancer Chemoresistance and Progression through Twist Activation. Molecular cell. 2016;63(6):1021–33.
38. Wang M, Chen X, Chen H, Zhang X, Li J, Gong H, Shiyan C, Yang F. RNF8 plays an important role in the radioresistance of human nasopharyngeal cancer cells in vitro. Oncol Rep. 2015;34(1):341–9.
39. Zhao MJ, Song YF, Niu HT, Tian YX, Yang XG, Xie K, Jing YH, Wang DG. Adenovirus-mediated downregulation of the ubiquitin ligase RNF8 sensitizes bladder cancer to radiotherapy. Oncotarget. 2016;7(8):8956–67.

Figures

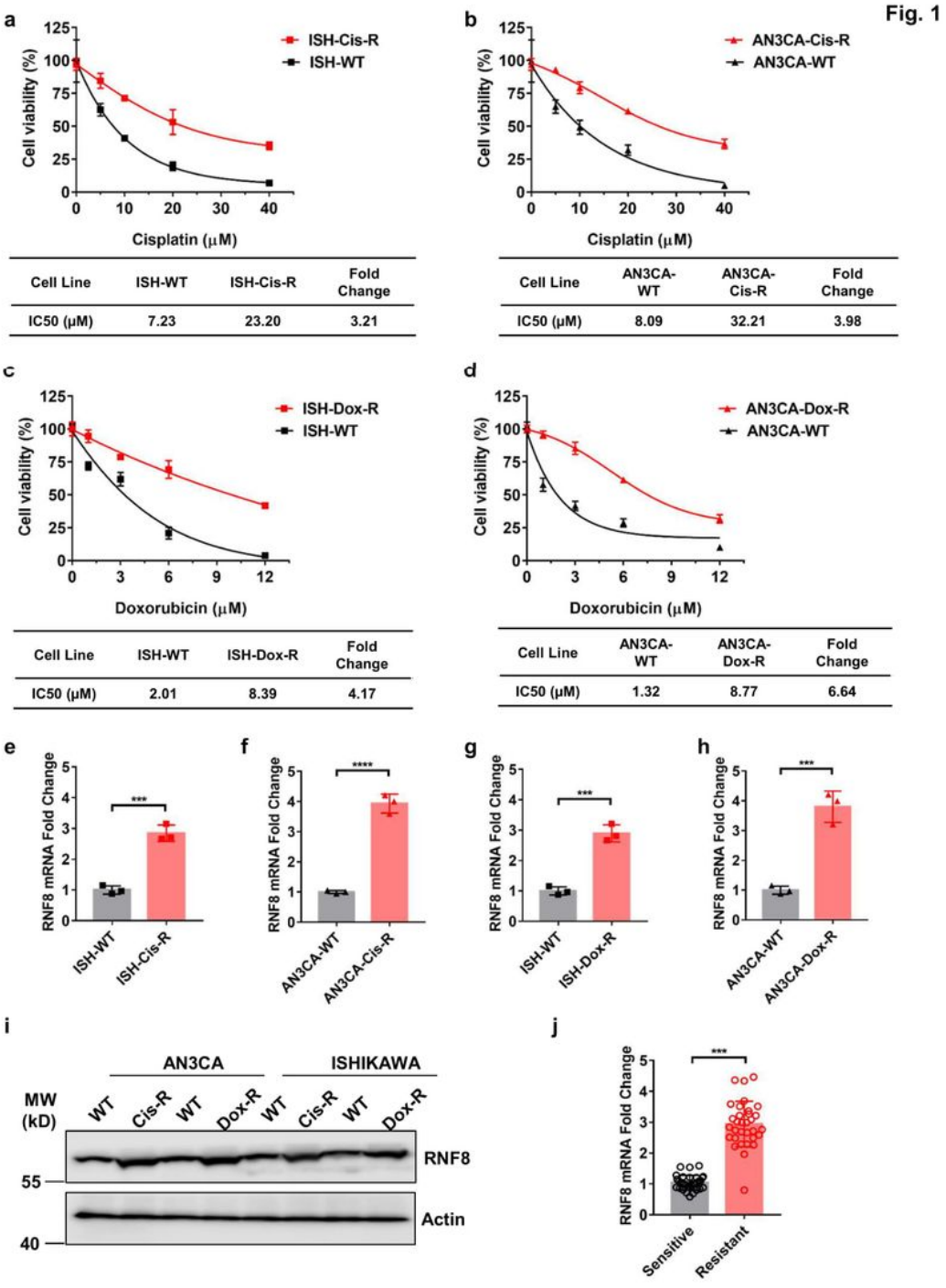

Cell Line	ISH-WT	ISH-Cis-R	Fold Change
IC50 (μM)	7.23	23.20	3.21

Cell Line	AN3CA-WT	AN3CA-Cis-R	Fold Change
IC50 (μM)	8.09	32.21	3.98

Cell Line	ISH-WT	ISH-Dox-R	Fold Change
IC50 (μM)	2.01	8.39	4.17

Cell Line	AN3CA-WT	AN3CA-Dox-R	Fold Change
IC50 (μM)	1.32	8.77	6.64

Figure 1

Expression of RNF8 is increased in cisplatin and doxorubicin resistant EC cells. a Cell viability of ISH-WT, ISH-Cis-R, b AN3CA-WT and AN3CA-Cis-R cells. Cisplatin concentrations are 0 μM, 5 μM, 10 μM, 20 μM, and 40 μM. Data are represented as mean ± standard deviations (SD) of three independent experiments. c Cell viability of ISH-WT, ISH-Dox-R, d AN3CA-WT and AN3CA-Dox-R cells. Doxorubicin concentrations are 0 μM, 1 μM, 2 μM, 4 μM, and 8 μM. Data are represented as mean ± SD of three independent experiments.

e RNF8 mRNA expression in ISH-WT, ISH-Cis-R, f AN3CA-WT, AN3CA-Cis-R, g ISH-WT, ISH-Dox-R, h AN3CA-WT and AN3CA-Dox-R cells. ***: P<0.001. i Western blotting analysis of RNF8 protein expression in ISH-WT, ISH-Cis-R, AN3CA-WT and AN3CA-Cis-R, ISH-WT, ISH-Dox-R, AN3CA-WT and AN3CA-Dox-R cells. j RNF8 mRNA expression in EC patient samples. platinum sensitive group: n=32. platinum resistant group: n=32. ***: p<0.001.

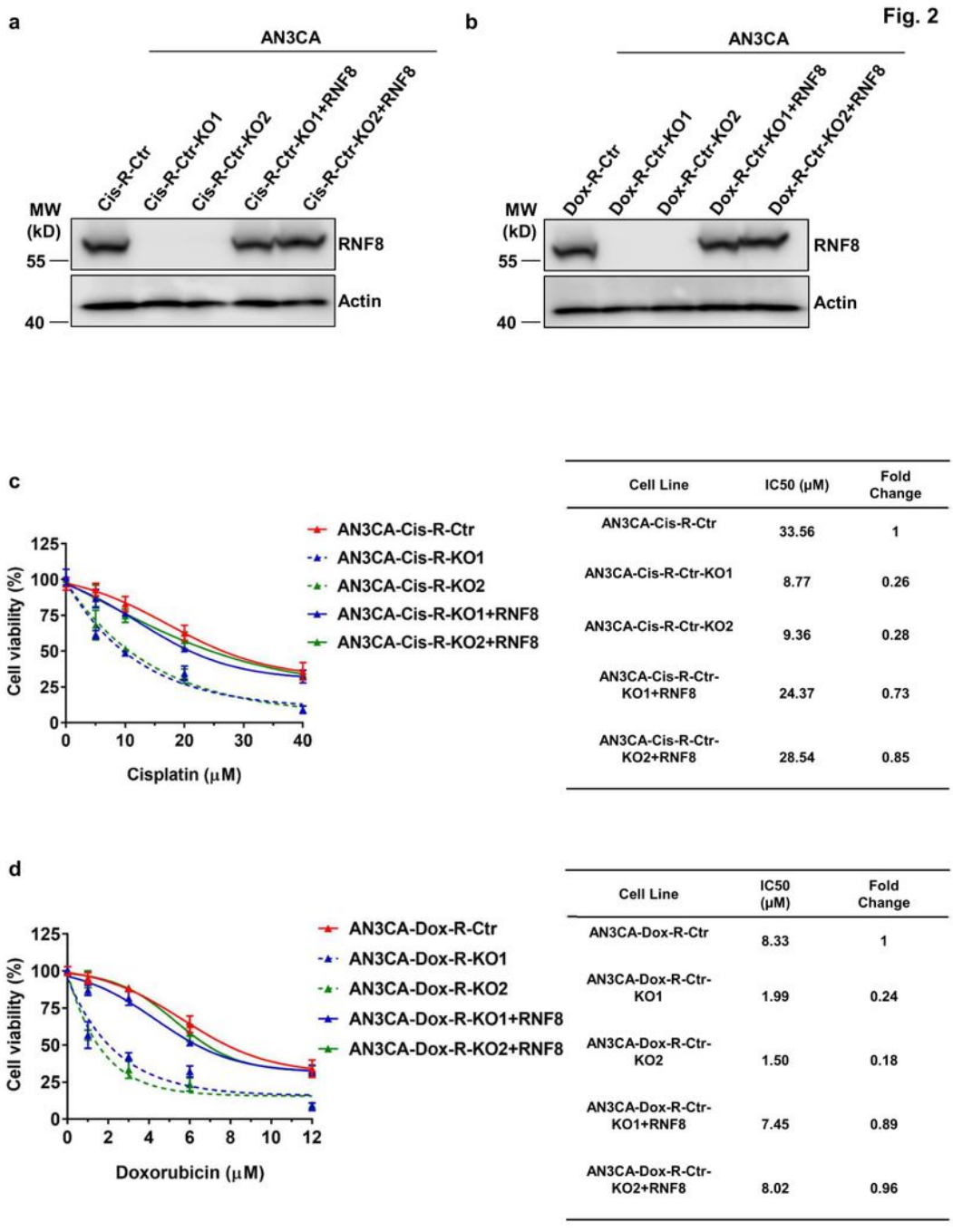

Cell Line	IC50 (μM)	Fold Change
AN3CA-Cis-R-Ctr	33.56	1
AN3CA-Cis-R-Ctr-KO1	8.77	0.26
AN3CA-Cis-R-Ctr-KO2	9.36	0.28
AN3CA-Cis-R-Ctr-KO1+RNF8	24.37	0.73
AN3CA-Cis-R-Ctr-KO2+RNF8	28.54	0.85

Cell Line	IC50 (μM)	Fold Change
AN3CA-Dox-R-Ctr	8.33	1
AN3CA-Dox-R-Ctr-KO1	1.99	0.24
AN3CA-Dox-R-Ctr-KO2	1.50	0.18
AN3CA-Dox-R-Ctr-KO1+RNF8	7.45	0.89
AN3CA-Dox-R-Ctr-KO2+RNF8	8.02	0.96

Figure 2

Depletion of RNF8 sensitize cisplatin and doxorubicin resistant EC cells. a Western blotting analysis of RNF8 protein expression in AN3CA-Cis-R-Ctr, RNF8 knockout AN3CA-Cis-R clone 1 (AN3CA-Cis-R-KO1), RNF8 knockout AN3CA-Cis-R clone 2 (AN3CA-Cis-R-KO2), RNF8 ectopic expressed AN3CA-Cis-R-KO1 (AN3CA-Cis-R-KO1+RNF8), RNF8 ectopic expressed AN3CA-Cis-R-KO2 (AN3CA-Cis-R-KO2+RNF8), b AN3CA-Dox-R-Ctr, RNF8 knockout AN3CA-Dox-R clone 1 (AN3CA-Dox-R-KO1), RNF8 knockout AN3CA-Dox-R clone 2 (AN3CA-Dox-R-KO2), RNF8 ectopic expressed AN3CA-Dox-R-KO1 (AN3CA-Dox-R-KO1+RNF8), RNF8 ectopic expressed AN3CA-Dox-R-KO2 (AN3CA-Dox-R-KO2+RNF8) cells. c Cell viability of AN3CA-Cis-R-Ctr, AN3CA-Cis-R-KO1, AN3CA-Cis-R-KO2, AN3CA-Cis-R-KO1+RNF8 and AN3CA-Cis-R-KO2+RNF8 cells to cisplatin. Data are represented as mean ± SD of three independent experiments. d Cell viability of AN3CA-Dox-R-Ctr, AN3CA-Dox-R-KO1, AN3CA-Dox-R-KO2, AN3CA-Dox-R-KO1+RNF8, AN3CA-Dox-R-KO2+RNF8 cells to doxorubicin. Data are represented as mean ± SD of three independent experiments.

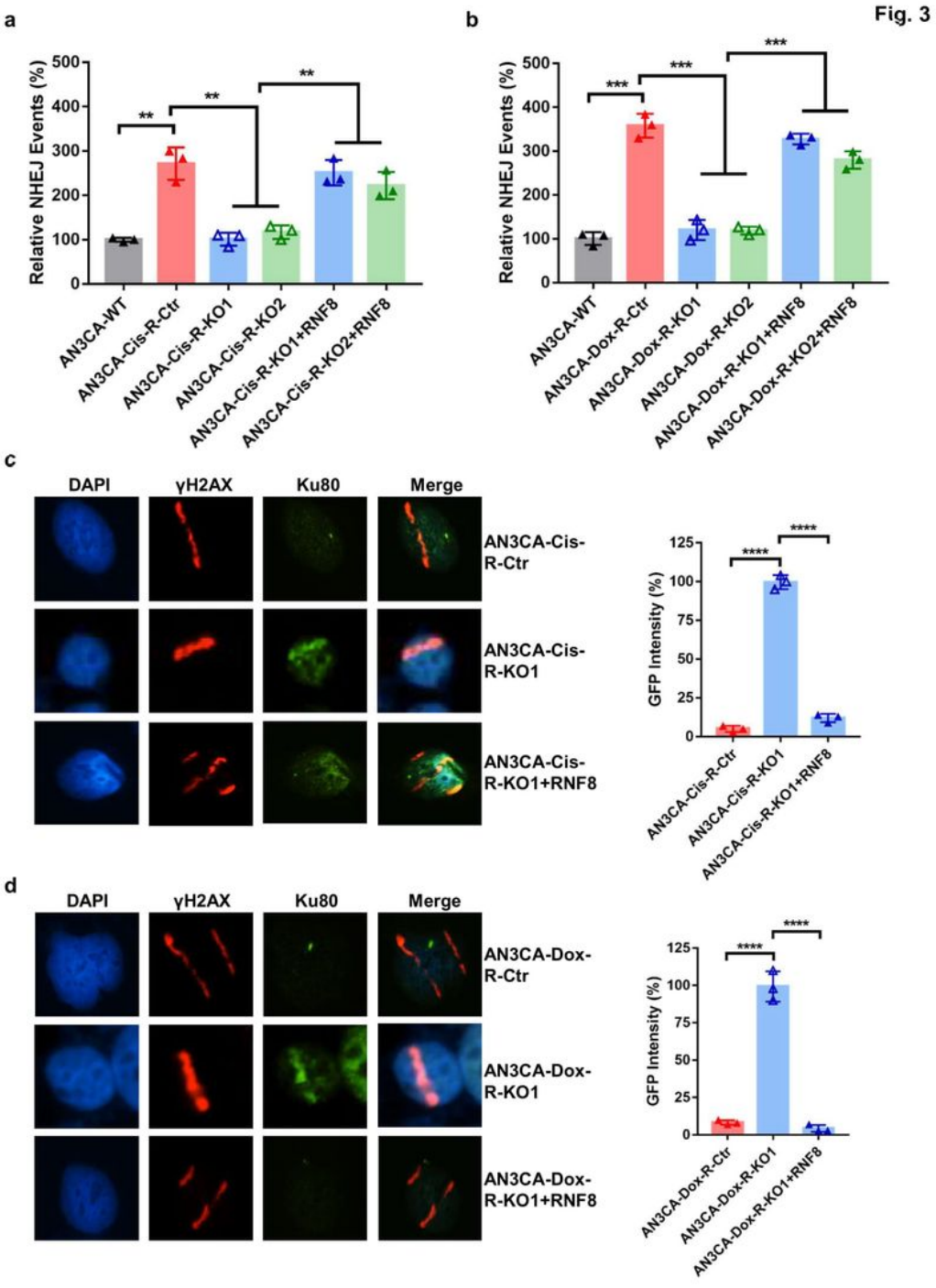

Figure 3

RNF8 deficiency reduces NHEJ efficiency in cisplatin and doxorubicin resistant EC cells. a Relative NHEJ events in AN3CA-Cis-R, AN3CA-Cis-R-KO1, AN3CA-Cis-R-KO2, AN3CA-Cis-R-KO1+RNF8 and AN3CA-Cis-R-KO2+RNF8 cells. Data are represented as mean ± SD of three independent experiments. **: P<0.01. b Relative NHEJ events in AN3CA-Dox-R, AN3CA-Dox-R-KO1, AN3CA-Dox-R-KO2, AN3CA-Dox-R-KO1+RNF8, AN3CA-Dox-R-KO2+RNF8 cells. Data are represented as mean ± SD of three independent experiments. ***:

P<0.001. c Localization of Ku80 at DNA damage sites upon DNA damage in AN3CA-Cis-R-Ctr, AN3CA-Cis-R-KO1 and AN3CA-Cis-R-KO1+RNF8 cells. Cells were subjected to immunofluorescent staining 4 h after exposure to microirradiation. ****: P<0.0001. d Localization of Ku80 at DNA damage sites upon DNA damage in AN3CA-Dox-R-Ctr, AN3CA-Dox-R-KO1 and AN3CA-Dox-R-KO1+RNF8 cells. Cells were subjected to immunofluorescent staining 4 h after exposure to microirradiation. ****: P<0.0001.

Fig. 4

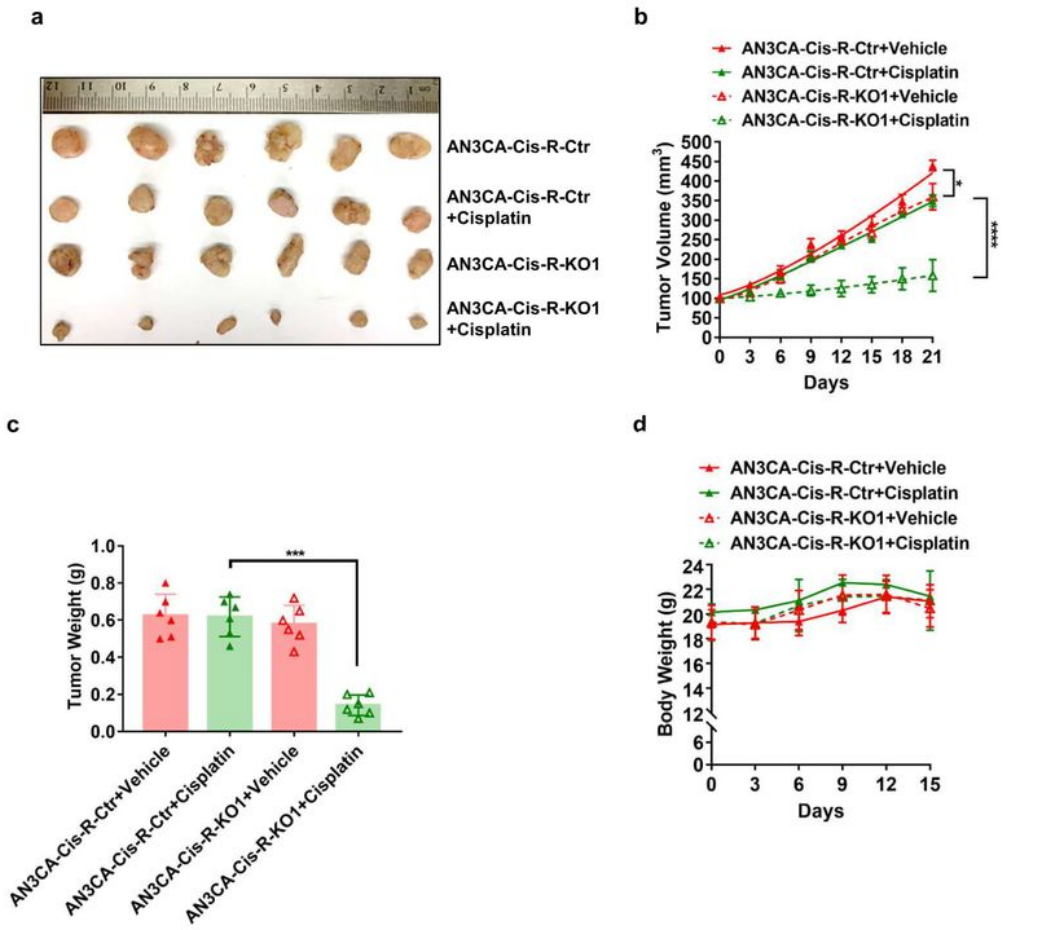

Figure 4

Inhibition of RNF8 increases sensitivity to cisplatin in vivo. a Photograph of tumors dissected from mice at day 21 in AN3CA-Cis-R-Ctr and AN3CA-Cis-R-KO1 xenograft. Female BALB/c nude mice were treated intraperitoneally with vehicle (DMSO) or cisplatin (8 mg/kg/3days). Group size: 6 mice/group. b Tumor growth, c Tumor size and d body weight of AN3CA-Cis-R-Ctr and AN3CA-Cis-R-KO1 xenograft in response to cisplatin. *: $p<0.05$, ****: $p<0.0001$.